

PAPER • OPEN ACCESS

Features of focusing magnetoelastic waves in YIG crystals

To cite this article: S M Bakharev *et al* 2019 *J. Phys.: Conf. Ser.* **1389** 012096

View the [article online](#) for updates and enhancements.



IOP | ebooks™

Bringing together innovative digital publishing with leading authors from the global scientific community.

Start exploring the collection—download the first chapter of every title for free.

Features of focusing magnetoelastic waves in YIG crystals

S M Bakharev^{1,2*}, M A Borich^{1,2}, S P Savchenko¹

¹M.N. Miheev Institute of Metal Physics, Ekaterinburg, Russia

²Ural Federal University, Ekaterinburg, Russia

E-mail: bakharevsm@imp.uran.ru

Abstract. The focusing features and caustic of magnetoelastic waves in $\text{Y}_3\text{Fe}_5\text{O}_{12}$ (YIG) crystals in the long wavelength approximation are investigated. It is shown that the interaction of phonon and magnetic subsystems leads to pronounced anisotropic properties of magnetoelastic waves. Four magnetoelastic eigenmodes are realized in the crystal, and two of them possess a focusing and caustic in the vicinity of magnetoelastic resonance point. The region of frequencies and wavenumbers of magnetoelastic waves is obtained, where the caustic can be observed. The directions of the focusing and caustic are defined.

1. Introduction

The possibility of using magnetic waves in magnetic ordered media in a number of technical devices is due to the unique properties of these waves. $\text{Y}_3\text{Fe}_5\text{O}_{12}$ (YIG) is one of the well studied compounds that has been used in electronic devices for a number of decades. The main property of YIG is a narrow line of ferromagnetic resonance (FMR) and a small value of spin wave dissipation in the vicinity of FMR [1]. Elastic waves can also propagate through a YIG crystal, and these waves are almost isotropic. The elastic properties of YIG are well known [2]. Despite the fact that the magnetoelastic properties of YIG crystals have been studied in detail both experimentally and theoretically [3, 4], however, until now, the effects of focusing and caustics of magnetoelastic waves have not been considered. The purpose of this paper is to take into account the interaction between these two well known subsystems and to investigate the peculiarities of magnetoelastic waves propagation. As it is shown in the paper, the group and phase velocities of magnetoelastic waves in YIG are non-collinear, and it leads to the appearance of preferred directions in the crystal. Thus, the focusing of magnetoelastic waves can be observed in some directions and the defocusing in some other directions. The intensity of the waves propagating along a specific direction in the focusing region increases sharply. This phenomena is called a caustic. Note that the light caustic is a well known phenomenon, while magnetoelastic caustic is a new one [5]. In this paper we investigate the focusing and caustic of magnetoelastic waves. Their spectrum is obtained in long wavelength approximation [6, 7, 8, 9, 10]. The frequency and wavenumber regions where the caustic can be observed are determined, and the directions of the caustic at the corresponding frequency are defined as well.



2. Model

Let us obtain the spectrum of magnetoelastic waves in the framework of the macroscopic theory of the magnon-phonon interaction in the ferromagnetic dielectric YIG, which has a cubic lattice [6, 7, 8, 9, 10]. The energy consists of the elastic part in the harmonic approximation

$$W_e = \frac{1}{2}(e_{yy}^2 + e_{zz}^2 + e_{xx}^2)c_{11} + (e_{xx}e_{yy} + e_{xx}e_{zz} + e_{yy}e_{zz})c_{12} + (2e_{xy}^2 + 2e_{xz}^2 + 2e_{yz}^2)c_{44}, \quad (1)$$

where c_{11} , c_{12} and c_{44} are the second order elastic modules, and $e_{ij} = (\partial u_i / \partial x_j + \partial u_j / \partial x_i) / 2$ is the symmetric deformation tensor, the magnetoelastic part is assumed to be due to the magnon-phonon interaction

$$W_{me} = (M_x^2 e_{xx} + M_y^2 e_{yy} + M_z^2 e_{zz}) \frac{b_1}{M_0^2} + (M_x M_y e_{xy} + M_x M_z e_{xz} + M_y M_z e_{yz}) \frac{b_2}{M_0^2}, \quad (2)$$

where b_1 , b_2 are the magnetoelastic constants, M_i are the magnetization components of the vector \mathbf{M} , M_0 is the saturation magnetization, and the magnetic energy is given by

$$W_m = \frac{A_{ex}}{M_0^2} (\nabla \mathbf{M})^2 - (\mathbf{M}, \mathbf{H}), \quad (3)$$

where A_{ex} is the exchange coupling constant and \mathbf{H} is the external magnetic field. The cubic anisotropy of YIG samples with spinel structure is small enough and can be neglected in this research. All magnetic parameters of YIG are well known: coupling parameter is equal to $A_{ex} = 4.3 \cdot 10^{-7} \text{ erg} \cdot \text{cm}^2$, saturation magnetization $4\pi M_0 = 1750 \text{ Oe}$, and magnetoelastic parameter $b_2/M_0^2 = 225$ [11]. The typical value of external magnetic field is about $H = 10^3 \text{ Oe}$. The elastic constants of YIG are also known: $c_{11} = 2.69 \cdot 10^{12} \text{ dyn/cm}^2$, $c_{44} = 0.764 \cdot 10^{12} \text{ dyn/cm}^2$, and $c_{12} = 1.077 \cdot 10^{12} \text{ dyn/cm}^2$ [2]. The elastic anisotropy parameter of YIG crystal is equal to $k - 1 = (c_{12} + c_{44}) / (c_{11} - c_{44}) \approx -0.04$, and YIG can be considered almost isotropic therefore. It allows to use isotropic approximation ($k - 1 = 0$) further. In this paper, we restrict ourselves the consideration of magnetoelastic waves in the long wavelength approximation. Thus, the equations of motion are given by

$$\rho \ddot{u}_i = \frac{\partial \sigma_{ik}}{\partial x_k}, \quad \dot{\mathbf{M}} = -\gamma_e [\mathbf{M}, \mathbf{H}_{eff}], \quad (4)$$

where $\rho = 5.7 \text{ g/cm}^3$ is the density of YIG, $\sigma_{ik} = \partial W / \partial e_{ik}$ is the stress tensor, u_i is the elastic displacement, $\gamma_e = 2.8 \cdot 10^6 \text{ Oe}^{-1} \text{ s}^{-1}$ is the giromagnetic ratio, and $\mathbf{H}_{eff} = -\delta W / \delta \mathbf{M}$ is the effective magnetic field. Note that the dissipation is usually very small in YIG: the typical FMR linewidth in the experiments with the spin waves in YIG films is about 0.1-1 Oe at the frequency region 1-10 GHz (external magnetic field of about 1-3 kOe) [4, 12, 13]. Thus, we neglected the dissipation term.

Let us apply an external magnetic field \mathbf{H} along the z axis. Since both anisotropy and magnetoelastic interaction in our problem are assumed to be small, the saturation magnetization \mathbf{M} should also be directed along the z axis. The linear approximation of the equation of motion represents the homogeneous set of 5 linear equations with respect to u_x , u_y , u_z , M_x , and M_y , and the condition for the existence of linear magnetoelastic waves with the wavenumber \mathbf{q} and the frequency ω is given by the equation $F(\mathbf{q}, \omega, \theta) = 0$, where F is the determinant of the system. The terms proportional to the constant b_1 disappear in this approximation. In this approach, therefore, there remains only one parameter b_2 which describes the phonon-magnon

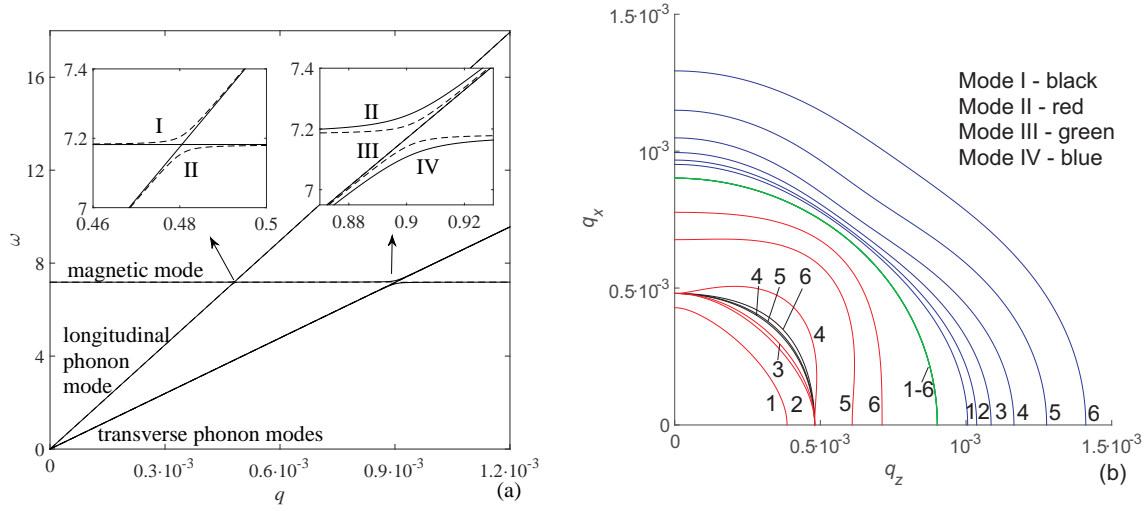


Figure 1. (a) The spectrum of magnetoelastic waves. Solid lines are the $\omega(q)$ dependencies for $\theta = 0$ and dash lines are the eigenmodes for $\theta = \pi/4$. (b) The constant frequency levels $q(\theta)$ in (q_x, q_z) plot in the vicinity of resonance points. Lines 1-6 correspond to $\delta = -5 \cdot 10^{-4}$, $\delta = -3 \cdot 10^{-4}$, $\delta = -10^{-4}$, $\delta = 10^{-4}$, $\delta = 3 \cdot 10^{-4}$, and $\delta = 5 \cdot 10^{-4}$ respectively. The frequency and wavevector are given in dimensionless form: $\omega \rightarrow \omega/(\gamma_e M_0)$, and $q \rightarrow qa$.

interaction. Magnetoelastic constant is equal to $b_2/M_0^2 = 225$ for YIG crystal [11]. Note that if the anisotropy is supposed to be equal to zero ($k - 1 = 0$), then determinant of the system is independent on polar angle ϕ . Thus, all of the properties of magnetoelastic waves can be obtained from the $\{010\}$ plane consideration.

3. Results

The purpose of this paper is to investigate the conditions of the magnetoelastic wave focusing. Let us note some properties of spectrum of these waves. There are four eigenfrequencies for any value of wavenumber q . At the small values of q the lower two modes represent the transverse elastic waves (modes III and IV in the figure 1 (a)), the next one is the longitudinal elastic wave (mode II) and the highest one is the magnetic mode (I). With the increasing q , the longitudinal elastic mode reaches the magnetic one, and the first magnetoelastic resonance point appears. In the vicinity of this point the behavior of the modes depends on the angle θ . In particular, for $[100]$ direction ($\theta = 0$) the magnetic and longitudinal elastic modes cross each other, while for $[101]$ direction ($\theta = \pi/4$) the situation is different. The elastic mode curves and transforms into a magnetic one, and magnetic mode, respectively, becomes elastic. It is shown in the left inclusion in the figure 1 (a): the solid lines I and II corresponding to $\theta = 0$ cross each other, and the dashed lines I and II corresponding to $\theta = \pi/4$ repel each other. With further wavenumber increasing the frequency of transfer waves reaches the frequency of magnetic mode and the second magnetoelastic resonance point appears. At this point, the magnetic mode is transformed into a transverse elastic mode, and one of the two elastic modes transforms to a magnetic mode, and the second elastic mode remains elastic. The different propagation directions correspond to the different value of gap between the modes at the resonance point. This feature is shown in the figure 1 (a). Note that the wavenumbers and frequencies in the figure 1 are given in dimensionless form for the convenience: $q \rightarrow qa$, where $a = 1.2376 \cdot 10^{-7}$ cm is the YIG lattice parameter and $\omega \rightarrow \omega/(\gamma_e M_0)$. Note also that the magnetic mode is proportional to the square of q while the elastic modes increases linearly. It means that the two more resonance points

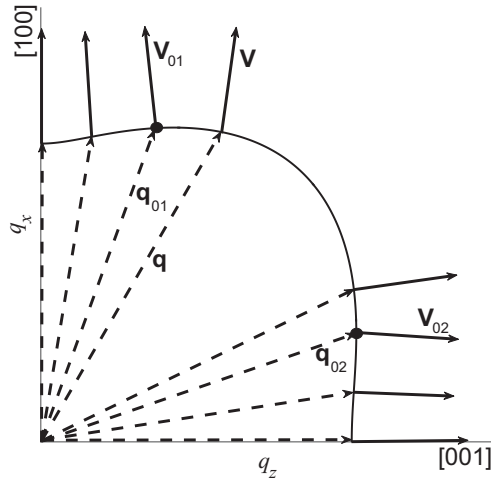


Figure 2. Illustration of the magnetoelastic waves focusing along the [100] and [001] directions. The solid line is a constant frequency line on (q_x, q_z) plot. Bold points (•) corresponding to the zero curvature ($K(\mathbf{q}_{0(1,2)}) = 0$) refer to the caustics. The wavevector \mathbf{q} and corresponding group velocity vector \mathbf{V} of the magnetoelastic wave are shown in the figure.

exists but these points correspond to the large value of q and extremely high frequencies and our continuous medium model can not be applied for such situation.

The analysis of spectrum shows that the dependence of wave properties on the direction can be observed in the small vicinity of resonance points only. The most brightly expressed way to demonstrate this dependence is the investigation of constant energy lines. The figure 1 (b) shows the set of lines $q(\theta)$ corresponding to the frequencies $\omega = \gamma_e H(1 + \delta)$, where $\delta = (-5, -3, -1, 1, 3, 5) \cdot 10^{-4}$. The group of lines in the figure 1 (b) is structured in accordance to the above mentioned mode classification. The group of black lines (I) is a magnetic mode, which, after crossing the first resonance point, turns into an elastic one. This mode exists for positive δ only and remains almost isotropic. The set of red lines (II) in the figure 1 (b) corresponds to a mode that turns from elastic to magnetic at the first resonance point and again into an elastic at the second resonance point. This group exists both for positive and negative δ and demonstrates the anisotropy in a specific region of δ . The transformation of the lines of the group (II) is as follows. The lines remain almost isotropic for negative δ but the absolute value of q increases when δ changes from $-5 \cdot 10^{-4}$ to $-3 \cdot 10^{-4}$. Then for the values of δ from $-3 \cdot 10^{-4}$ to $+1 \cdot 10^{-4}$ the situation becomes more complicated. The wavevector q save it's length at the [100] ($\theta = \pi/2$) and [001] ($\theta = 0$) directions, but the wavenumber becomes substantially larger at other directions and anisotropy of the mode is brightly expressed. The further increasing in frequency leads to an increase in the wavenumber in all directions, and anisotropy decreases therefore. The group of constant energy lines (III) (green lines in the figure 1 (b)) is an elastic mode that does not transform when it crosses a resonance point. It is an isotropic mode. The last group of lines (IV) represents the mode, which transforms from a transverse elastic mode into a magnetic one at the second resonance point. It shows a small anisotropy for small positive δ and becomes isotropic for large δ .

Further analysis is based on a detailed study of the properties of constant energy surfaces at frequencies close to the magnetoelastic resonance. The group velocity is perpendicular to these surfaces, and peculiarities on the surface are responsible for the specific features of wave propagation. An illustrative diagram of the phenomenon of magnetoelastic waves focusing along the [001] and [100] directions is shown in the figure 2. In the vicinity of these directions, the group velocities \mathbf{V} deviate from the wave vector \mathbf{q} to the corresponding focusing directions.

It was shown [14, 15] that the ratio of the spin wave flux density in a specific direction to spin wave flux density in an isotropic medium is equal to $A(\omega, \theta) = V_n / (V K(\omega, \theta) q^2)$, where $K(\omega, \theta)$ is the Gaussian curvature of the surface of constant frequency ω , V is the group velocity magnitude, and V_n is it's component perpendicular to the surface $\omega(q, \theta) = const$. A is called amplification factor. The formula for amplification factor is simplified in the case of YIG since

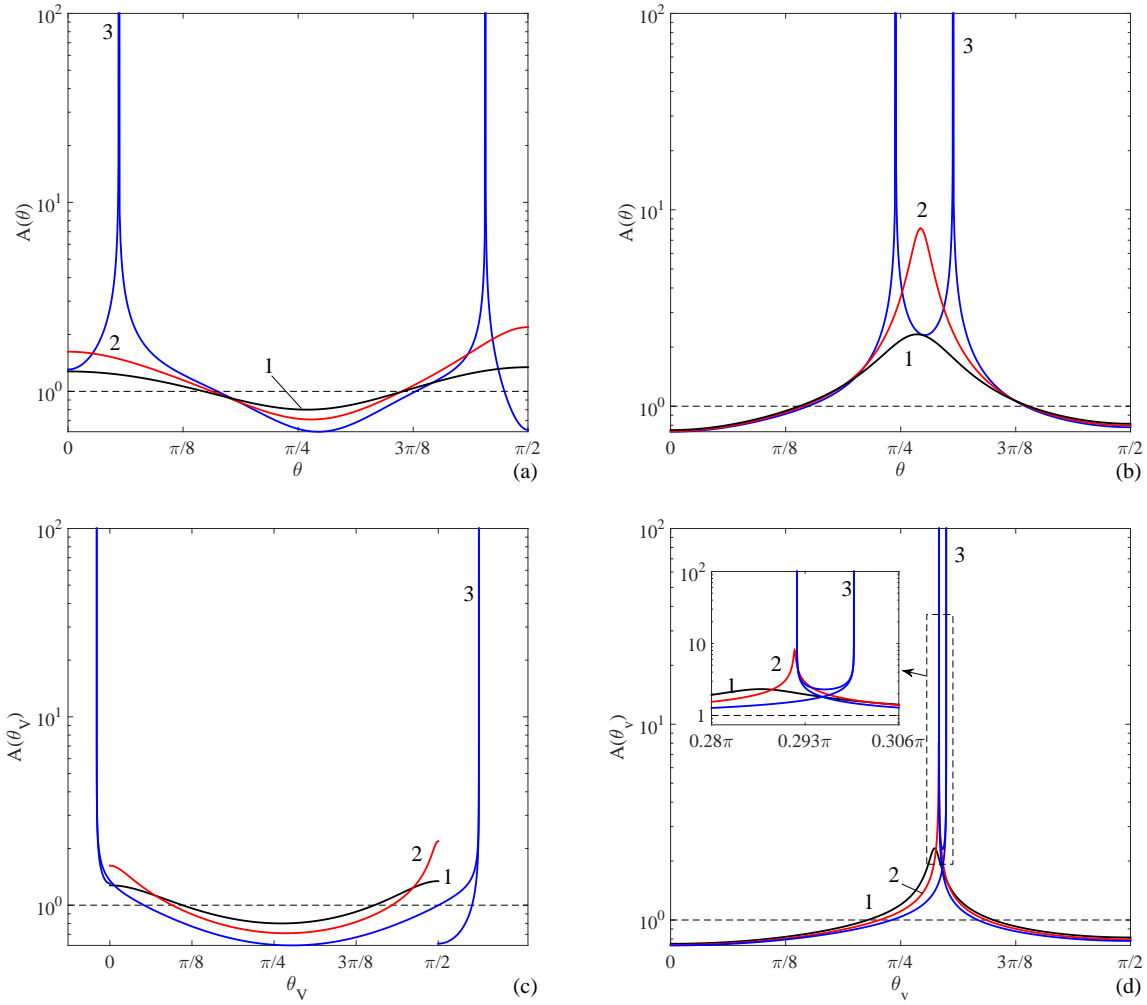


Figure 3. The dependencies of the amplification factor of modes II (a,c) and modes IV (b,d) on the angle θ (a,b) and on the angle θ_V (c,d) in the vicinity of resonance frequency $\omega = \gamma_e H(1 + \delta)$. Black curves 1 correspond to $\delta = -1 \cdot 10^{-4}$, red curves 2 correspond to $\delta = 0$, and blue curves 3 refer to $\delta = 1 \cdot 10^{-4}$. Direct dashed lines are isotropic case ($A = 1$).

all physically different situations can be obtained from $\{010\}$ plane, where $\phi = 0$ and one can use plane curvature instead of Gaussian. As it was shown, all significant transformations of the surface occur in the vicinity of frequency $\omega = \gamma_e H$ and on the modes defined as II and IV in the figure 1 (b). The curvature of these surfaces has to be considered precisely. The result is as follows. The curvature of mode II is positive for $\delta < 0$, but the dependence $K(\theta)$ becomes stronger when δ increases from $-5 \cdot 10^{-4}$ to zero. When δ is positive, but small enough ($\delta = 10^{-4}, 3 \cdot 10^{-4}$), the behavior of the surface changes. A part of the curve becomes concave, and the inflection points appear at angles θ close to zero and $\pi/2$. These are points of zero curvature and the amplification factor tends to infinity at these points. In other words, the caustic of magnetoelastic waves is realized. With further increasing of δ the line $q(\theta)|_{\omega=\text{const}}$ becomes convex everywhere again and the caustic vanishes. The situation is similar to the set of modes IV. For large negative δ , the curvature $K(\omega, \theta)$ slightly depends on the angle θ , but the dependence is significant when $\delta \rightarrow 0$. For small positive values δ , the concave part of curve $q(\theta)|_{\omega=\text{const}}$ appears near the angle $\theta = \pi/4$ and the caustic of these waves can be observed at

angles with $K(\omega, \theta_0) = 0$. The surface is close to isotropic one when $\delta \geq 5 \cdot 10^{-4}$. The caustic position can be determined by examining the dependencies of amplification factor on angle θ_0 shown in the figure 3. For a non-positive δ the dependence $A(\theta)$ is a smooth function both for mode II and mode IV (lines 1 and 2 in the figure 3 (a,b)). For small positive δ ($\delta = 10^{-4}$, lines 3) the second order discontinuances appear at the angles close to 0 and $\pi/2$ for mode II and at the angles close to $\pi/4$ for mode IV. The positions of these discontinuances determine the caustic directions. The dashed horizontal line in the figure 3 corresponds to the isotropic propagation of the waves ($A = 1$). The regions of plot $A(\theta)$ above the dashed line refer to the focusing of the wave while the regions below corresponds to the defocusing.

Note that the angle θ determines the direction of wavevector \mathbf{q} that differs from the direction of group velocity \mathbf{V} . The propagation of energy is determined by the group velocity and the direction of focusing and caustic should be defined through the direction of \mathbf{V} therefore. The azimuthal angle θ_V of the group velocity is linked to the angle θ of wavevector by the simple relation $\theta_V = \theta + \arctan(V_\theta/V_n)$, where $V_\theta = q^{-1}\partial\omega/\partial\theta$ and $V_n = \partial\omega/\partial q$ are the group velocity components in spherical set of coordinates. The angular dependencies $A(\theta_V)$ of amplification factor in V -space are shown in the figure 3 (c,d). The caustic directions in V -space become slightly outside the interval $(0, \pi/2)$ for mode II (see figure 3 (c)), while two directions of mode IV caustic become close to each other (see figure 3 (d) and inclusion in it).

Note that according to the definition the amplification factor is equal to the ratio of the spin waves flux density in a specific direction to spin waves flux density in an isotropic medium. The infinite value of amplification factor in the caustic direction means the infinite value of spin waves flux density in this direction. Any physical characteristic of spin waves (flux, energy etc.) is equal to the integral of this density over the corresponding spatial angle and remains finite therefore. Note also that the taking into account the dissipation changes the caustic picture in some details but does not lead to principal differences. The directions with infinite value of amplification factor will be slightly shifted due to dissipation, but the value of A remains infinite. Caustic is a geometric property of the constant energy surface and this surface retains its properties, at least when the dissipation is sufficiently small.

4. Conclusions

In this paper, based on the analysis of constant frequency surfaces, the focusing conditions and caustic of magnetoelastic waves in a YIG crystal are investigated. The elastic subsystem of the YIG crystal is almost isotropic ($c_{12} \approx c_{11} - 2c_{44}$), and the anisotropy of the waves is due to the magnetoelastic interaction. Two of the four magnetoelastic eigenmodes have important peculiarities in the vicinity of the point of magnetoelastic resonance. The constant energy surfaces of these modes contain both the convex and concave regions and the caustic conditions are satisfied at the points of zero curvatures of these surfaces. The isotropy of elastic and magnetic subsystems tends to the independence of eigenfrequencies on the polar angle ϕ . It was shown that the caustic is realized at the set of angles θ in the $\{010\}$ plane. The symmetry with respect to the rotation around z axis tends to the conclusion that the directions of caustic forms the conical surfaces with corresponded conical angles θ . It is important that caustic can be observed in the region of frequencies and wavenumbers that can be reached in an experiment. For instance, the resonance frequency of YIG is equal to $\omega_r = 2.8 \cdot 10^9 \text{ s}^{-1}$ in the magnetic field $H = 10^3 \text{ Oe}$. Thus, the dimensionless shift $\delta = 10^{-4}$ from the resonance corresponds to the $\Delta\omega \sim 0.28 \cdot 10^6 \text{ s}^{-1}$ and can definitely be obtained in the experiment with the required accuracy. The corresponding wavenumbers are about $q_r = 7.28 \cdot 10^3 \text{ cm}^{-1}$ and also can be studied in the FMR experiment. Under these conditions, the caustic cones have the angles $\theta_0 = 4.94^\circ$ and $\theta_0 = 71.8^\circ$ for the mode IV, and $\theta_0 = 52.6^\circ$ and $\theta_0 = 53.7^\circ$ for the mode II. The caustic cones are well separated from each other, and a sharp increase in the intensity of magnetoelastic waves propagating in these directions can be studied experimentally.

Acknowledgments

The research was carried out within the state assignment of Minobrnauki of Russia (theme “Function” AAAA-A19-119012990095-0) and project No. 32-1.1.3.5 of the Program of Basic Research of the Presidium of the Russian Academy of Science, supported in part by RFBR (project No. 18-32-00139).

References

- [1] Spencer E G, Denton R T, Chambers R P 1962 *Phys. Rev.* **125** 1950
- [2] Clark A E, Strakna R E 1961 *Journ. Appl. Phys.* **32** 1172
- [3] LeCraw R C, Comstok R 1968 Magnetoelastic interactions in ferromagnetic dielectrics *Physical acoustics. Principles and Methods (Lattice Dynamics vol III, part B)* ed W P Mason (New York and London: Academic press) chapter 4 pp 127–199
- [4] Strauss W 1968 Magnetoelastic properties of yttrium ferrite garnet *Physical acoustics. Principles and Methods (Applications to Quantum and solid state physics vol IV, part B)* ed W P Mason (New York and London: Academic press) chapter 5 pp 211–264
- [5] Arnold V I 1990 *Theory of catastrophes* (Moscow: Nauka) [in Russian]
- [6] Smolensky G A, Iemanov V V, Nedlin G M, Petrov M P, Pisarev R V 1974 *Physics of magnetic dielectrics* (Leningrad: Nauka) p 284 [in Russian]
- [7] Turov E, Irkhin Yr 1956 *Metal Physics and Metallography* **3** 15 [in Russian]
- [8] Vlasov K 1965 *Metal Physics and Metallography* **20** 3 [in Russian]
- [9] Tiersten H F 1965 *Journ. Appl. Phys.* **36** 2250
- [10] Tucker J W, Rampton V W 1972 *Microwave ultrasonics in solid state physics* (Amsterdam: North-Holland publishing company) p 431
- [11] Lord A E 1968 *Phys. Kondens. Mater.* **7** 232
- [12] Syvorotka I I, Syvorotka I M, Ubizskii S B 2013 *Solid State Phenomena* **200** 250
- [13] Desvignes J, Mahasoro D, Gall H 1987 *IEEE Transactions on Magnetics* **230**(5) 3724
- [14] Bakharev S M, Savchenko S P, Tankeev A P 2019 *Physics of the Solid State* **61** 117
- [15] Maris H J 1971 *J. Acoust. Soc. Am.* **50** 812